Temperature and Solvent Effects on the Reactions of *o*-Positronium with Nitroso Spin Traps in Methanol−Water Mixed Solvents

Béla Lévay* and Márton Boros

Department of Nuclear Chemistry, Eötvös Loránd University, Budapest, Hungary

Received: December 11, 2003; In Final Form: February 19, 2004

Positron annihilation lifetime spectroscopy (PALS) is used to study the reactions of the *ortho*-positronium (*o*-Ps) atom with the following nitroso spin traps: nitrosobenzene (NOB), *N*,*N*-dimethyl-4-nitroso-aniline (DMNA), and *tert*-nitroso-butane (*t*-NOBu). The reaction rate constants (k) are close to the range that corresponds to that of diffusion-controlled reactions and exhibit a similar trend to those reported in the literature for the analogous nitro compounds. The differences between the aromatic and aliphatic nitroso and nitro compounds and the observed substituent effect are in good correlation with the calculated LUMO energies of the molecules. The nucleophilic *o*-Ps attacks the molecules at their electron deficient aromatic ring. Solvent effects on the reaction rates in methanol−water solvent mixtures exhibit a complex and solute-dependent nature. The reactions are strongly affected by solvent viscosity; however, the expected $1/\eta$ versus k variation is valid only for limited ranges of solvent compositions. The dielectric permittivity effect on the reaction rate constants does not follow the expected trend; k values in water are significantly greater than in the less polar methanol. The average activation enthalpies ($\Delta H^{\ddagger}$ and entropies ($\Delta S^{\ddagger}$) evaluated for the reaction of *o*-Ps with DMNA exhibit maxima at a solvent composition which corresponds to the most rigid solvent structure, where the activation energies of the transport processes such as viscosity and self-diffusion have extremes too. The validity of the isokinetic relation between $\Delta H^{\ddagger}$ and $\Delta S^{\ddagger}$ shows that the mechanism of the reaction of *o*-Ps does not depend on the solvent composition. $\Delta H^{\ddagger}$ exhibits an "Onsager reaction field" type $(\epsilon - 1)/(\epsilon + 2)$ dependence on solvent permittivity. The results are compared to literature data for the reactions of *o*-Ps with stable nitroxide free radicals and reaction of solvated electron with nitrobenzene (NO_2B) in methanol−water mixtures. The observed similarities and differences are discussed.

Introduction

Positronium (Ps) is the bound state of an electron and its antiparticle, a positron.[1−3] It is the simplest hydrogen-like exotic atom, and it can be considered as the lightest "0 mass number isotope" of hydrogen, where the heavy proton has been exchanged by the much lighter positron. Because of the different spin combinations of a positron and an electron, there are two possible Ps states, the *para*-Ps (*p*-Ps) with antiparallel (singlet) spin state and the *ortho*-Ps (*o*-Ps) with parallel (triplet) spin state. The intrinsic lifetimes of *p*-Ps and *o*-Ps are 0.125 and 140 ns, respectively.

When an energetic positron from a radioactive decay enters a condensed medium it will thermalize in a few picoseconds by losing its kinetic energy via ionization of the molecules of the medium creating a so-called ionization spur or track. The spur consists of electrons, positive ions, and excited molecules of the medium, radicals, and so forth. According to the basic idea of the spur model of positronium formation,[3,4] a thermalized positron can form a Ps atom with an electron, which is freed by the positron itself in its ionization spur.

Through its different decay modes, Ps can be used as an efficient microprobe of various physical or chemical properties of matter. In condensed medium, the long lifetime of *o*-Ps is shortened down to a few nanoseconds because of the so-called pick-off annihilation, whereby the positron in the *o*-Ps atom seeks out an electron in the surrounding molecules with opposite spin and annihilates with it instead of its own electron. No special chemical interactions between the *o*-Ps atom and the surrounding medium are involved in this process.

On the other hand, *o*-Ps atom can take part in various chemical reactions (e.g., substitution, oxidation, complex formation, etc.) with certain molecules of the system. Its annihilation characteristics will depend strongly on the physical and the chemical structure of these molecules. In solution, the chemical interactions (because of the increased proximity of electrons with opposite spin) will shorten the mean *o*-Ps lifetime as compared to the characteristic pick-off lifetime of the pure solvent. A special interaction of *o*-Ps is the so-called spin conversion reaction with paramagnetic molecules. In this process, because of the unpaired electron of the molecule, *o*-Ps is transformed to *p*-Ps, and its lifetime will be shortened accordingly. All these processes are called "quenching" of *o*-Ps. One of the most widely used experimental techniques to study the quenching of *o*-Ps is positron annihilation lifetime spectroscopy (PALS).

Certain groups of compounds such as diamagnetic nitroaromatics, electron deficient olefins such as maleic anhydride and quinones, and also nitriles proved to be very effective *o*-Ps quenchers.[5−7] All these molecules are known as good electron acceptors, and *o*-Ps reacts with them via donor−acceptor interaction.[8] The study of a series of substituted nitrobenzenes revealed a clear correlation between their reactivity and the Hammett's σ constant of the corresponding substituents.[8] It was also demonstrated that the positively charged carbon atoms of

* Corresponding author. E-mail: levay@para.chem.elte.hu.

10.1021/jp037804w CCC: $27.50
Published on Web 03/25/2004

SCHEME 1: Reaction of Nitrosobenzene with a Free Radical, Forming a Nitroxide

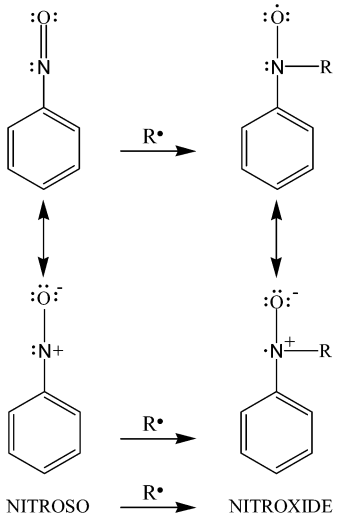

the benzene ring are the reactive centers where the nucleophilic *o*-Ps attacks the molecule.[5,9,10] Reaction of *o*-Ps with free radicals was also studied.[11−14]

A special group of free radicals, the stable nitroxides, was thoroughly investigated by Abbé and co-workers.[15] These compounds play a significant role in the study of biological systems by electron spin resonance (ESR) spectroscopy, using the so-called spin-labeling technique.[16] A molecule originally not bearing any unpaired electron is considered to be spin labeled when a nitroxide bearing molecule is covalently attached to it. Thus, it becomes possible to study this labeled molecule by the ESR technique.

An interesting branch of nitroxide chemistry is related to the "spin-trapping" method.[17] A variety of free radicals readily add to aromatic nitroso compounds and *tert*-nitrosoalkanes to give nitroxides. (See Scheme 1.) The scavenger properties of nitroso compounds leading to the formation of stable nitroxides can be utilized by the so-called nitroxide method for the identification of short-lived radicals otherwise not detectable by ESR spectroscopy.[17]

o-Ps, as a small radical, is expected to be easily trapped by nitroso spin traps and to possess high reactivity toward these molecules. Although nitroxides have already been investigated by the PALS technique,[15] we have not found any data for nitroso compounds. This prompted us to investigate the reaction of *o*-Ps with nitroso compounds and to compare the results with those found in the literature for nitroxides. Nitrosobenzene (NOB), *N*,*N*-dimethyl-4-nitroso-aniline (DMNA), and *tert*-nitroso-butane (*t*-NOBu) were chosen as spin traps. This selection of compounds makes it possible to study the substituent effect, the differences between aliphatic and aromatic systems, and thus to determine the structural characteristics of the molecules responsible for their reactivity.

In order to get more information about the factors affecting the rate and mechanism of the reaction, the aim of our work was to study the solvent and temperature effects in methanol−water mixtures. The solvent structure of alcohol−water mixtures can manifest itself in a large variety of physical properties, including viscosity, diffusion rates, and solvation properties of the reactants, dielectric properties of the medium, and so forth.[18]

Reactive Ps quenchers often show very high reactivity toward the solvated electron (e_s^-), and competing with positrons in the positron spur for capturing spur electrons can inhibit Ps formation. In this respect positronium chemistry and radiation chemistry results are interrelated and show several interesting correlations.[1−4] Therefore, it seems interesting to compare the reactions of *o*-Ps with nitroso spin traps to the reactions of the solvated electron with organic and charged solutes. The latter reactions were thoroughly investigated in methanol−water mixtures.[19−22]

Experimental Section

The nitroso compounds were obtained from Aldrich with 97% purity and were used without further purification. Solvent and temperature effects were investigated on the reactions of *o*-Ps with nitroso compounds. As the reactions are supposed to be diffusion controlled and thus strongly affected by the solvent viscosity, methanol (MeOH), water, and their mixtures were chosen as solvents, since the viscosity in these mixtures shows a very peculiar dependence on the solvent composition.[23] In the case of DMNA the measurements were carried out in the temperature range of 5−50 °C and in the whole composition range of the MeOH−water mixtures, NOB was studied also in the whole composition range of MeOH−water mixtures but only at 20 °C, whereas *t*-NOBu was studied in the temperature range of 5−60 °C but only in pure MeOH.

The positron annihilation lifetime spectra were recorded by a fast−fast coincidence spectrometer with BaF_2 scintillators. The time resolution of the setup was fwhm = 300 ps, and 10^6 counts were recorded in each spectrum. Three independent samples were prepared and measured for each concentration. The spectra were analyzed by the RESOLUTION computer program[24] in terms of three exponential components with lifetimes/decay rates $\tau_i = 1/\lambda_i$ and relative intensities I_i, where $i = 1, 2, 3$ corresponds to *p*-Ps, free positron, and *o*-Ps, respectively. The experimentally observed uncertainties of the results expressed as the standard deviations for the mean values of three independent measurements were only a little higher than the standard deviation of the individual measurements estimated by the RESOLUTION computer program.

The positron source consisted of about 1 MBq ^{22}Na thermally diffused into a sodium glass film of 2.5 mg/cm^2 thickness, resulting in a source correction of 9%. The source was fixed in an all-glass sample holder. The solution to be studied was thoroughly deoxygenated in the sample holder by pure nitrogen gas. A vacuum-tight Teflon screw stopper closed the sample holder, and the sample was kept under atmospheric pressure of nitrogen during the measurement. The holder was immersed in a thermostat, which was controlled with an accuracy of ±0.05 °C.

Results and Discussion

The rate constants (k) for the chemical reactions of *o*-Ps were calculated by the well-known eq 1[1] from the *o*-Ps decay rate constants (λ_3) measured as a function of the solute concentration (C):

$$\lambda_3(C) = \lambda_3(0) + kC \qquad (1)$$

$\lambda_3(C)$ and $\lambda_3(0)$ are the *o*-Ps decay rate constants measured in the solutions and in the pure solvent, respectively.

Effect of Chemical Structure. As examples, decay rate constants (λ_3) measured in MeOH at 20 °C are plotted as a function of the solute concentration for NOB, DMNA, and *t*-NOBu in Figure 1. The λ_3-C function has proved to be linear in all cases. The reaction rate constants (k) were calculated by eq 1 as the slopes of the least-squares-fit lines and are presented in Table 1.

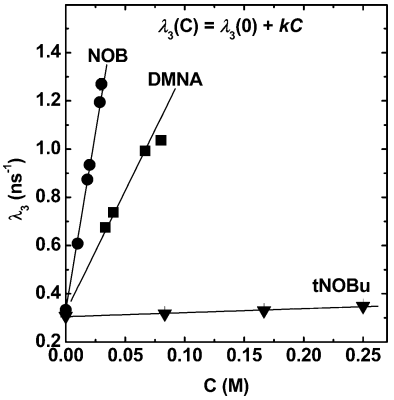

Figure 1. Decay rate constants of *o*-Ps atom (λ_3) are plotted as a function of solute concentration (●, NOB; ■, DMNA; ▼, *t*-NOBu) in MeOH at 20 °C. The reaction rate constants (k) were calculated by eq 1 as the slopes of the least-squares-fit lines and are presented in Table 1. (The experimentally observed uncertainties of λ_3 expressed as the standard deviations for the mean values of three independent measurements are less than the dimensions of the symbols for the data points in the figure.)

TABLE 1: Rate Constants of the Reactions of *o*-Ps with NOB, DMNA, and *t*-NOBu Measured in MeOH at 20 °C and Calculated LUMO Energies[25] of the Corresponding Nitroso Compounds[a]

nitroso compounds	k (10^9 M^{-1} s^{-1})	E_{LUMO} (eV)	nitro compounds	k (10^9 M^{-1} s^{-1})	E_{LUMO} (eV)
NOB	29.5 ± 0.7	−0.80	NO_2B	27.0 ± 2	−1.07
DMNA	10.3 ± 0.2	−0.51	$DMNO_2A$	18.0 ± 2	−0.94
t-NOBu	0.16 ± 0.02	+0.01	NO_2Pro	0.052 ± 0.002	+0.02

[a] For comparison, *o*-Ps rate constants with analogous nitro compounds measured in benzene at 20 °C[8], together with their calculated LUMO energies, are also presented (NO_2B, nitrobenzene; $DMNO_2A$, 3-nitro-*N*,*N*,-dimethylaniline; NO_2Pro, 1-nitropropane).

One can see that the aromatic nitroso compounds are much more reactive toward *o*-Ps than the aliphatic *t*-NOBu. For comparison, literature data of corresponding nitro compounds[8] are also shown in Table 1. Nitroso compounds exhibit an analogous trend to nitro compounds. Both the difference between the aromatic and aliphatic compounds and the effect of the dimethylamine substituent are similar for the two types of compounds. The reason for the high reactivity of the aromatic compounds can be attributed to the effect of electron withdrawing substituents, which make the aromatic system electron deficient and leads to low-lying LUMO orbitals. Hence, the nucleophilic *o*-Ps can effectively attack the molecules at their electron deficient aromatic ring. Electron-donating substituents, on the other hand, by decreasing the positive character of the ring decrease the reactivity of the molecule. We have calculated the LUMO energies of the nitro and nitroso compounds with the Gaussian 98[25] package at the AM1 level following a full geometry optimization. The results are presented in Table 1, and it is seen that LUMO energies correlate reasonably well with the rate constants in both groups of compounds.

Solvent Effects. The complete set of the rate constants for DMNA and NOB in MeOH−water mixtures measured at 20 °C is presented in Table 2 and plotted in Figure 2 together with the solvent viscosity data taken from the literature.[23] For comparison, the rate constants of the reaction of *o*-Ps with a nitroxide-type stable free radical HTMPO (4-hydroxy-2,2,6,6-tetramethylpiperidine-1-oxyl) measured in pure water and methanol at 20 °C[15] and the rate constants of the reaction of e_s^- with NO_2B measured in MeOH−water mixtures at 25 °C[21] are also shown in Figure 2. The *o*-Ps rate constants as a function

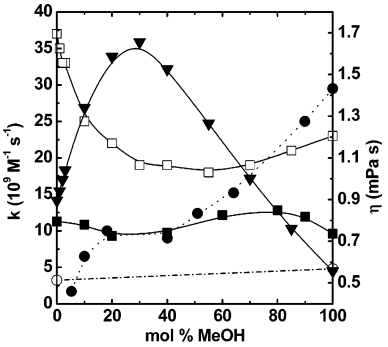

Figure 2. Solvent viscosity[23] (η, ▼) and rate constants (k) for reactions of *o*-Ps with NOB (●), DMNA (■), and HTMPO[15] (○) at 20 °C and of e_s^- with NO_2B[21] (□) at 25 °C in MeOH−water mixtures. The lines are visual fits, to guide the eye.

TABLE 2: *o*-Ps Reaction Rate Constants in MeOH−Water Mixtures at 20 °C and Average Activation Parameters in the Temperature Range of 5−50 °C

DMNA				NOB	
mol % MeOH	k (10^9 M^{-1} s^{-1})	$\Delta H^{\ddagger}$ (kJ/mol)	$\Delta S^{\ddagger}$ (J mol^{-1} K^{-1})	mol % MeOH	k (10^9 M^{-1} s^{-1})
0	11.3 ± 0.2	14.1 ± 0.9	5.7 ± 2.8	5	1.7 ± 0.2
10	10.9 ± 0.3			10	6.5 ± 0.3
20	9.3 ± 0.3	15.8 ± 0.4	8.1 ± 1.6	18	10.0 ± 0.3
40	9.7 ± 0.2	12.0 ± 0.7	−5.0 ± 0.3	40	9.0 ± 0.3
60	12.1 ± 0.2			51	12.4 ± 0.3
80	12.8 ± 0.3	5.4 ± 0.4	−23.9 ± 1.2	64	15.2 ± 0.4
90	11.9 ± 0.3			90	25 ± 0.3
100	9.6 ± 0.2	0.0 ± 0.3	−45.0 ± 0.9	100	29.5 ± 0.4

of the solvent composition show a quite complicated and complex solvent effect, which is even different for the two solutes. DMNA is relatively much less affected by the change of solvent composition as compared to NOB. The rate constant of HTMPO is somewhat higher in MeOH than in water.[15]

Similar complicated and solute-dependent solvent dependences have been reported for the reactions of solvated electrons with organic and charged solutes in MeOH−water mixtures.[20−22]

Solvent viscosity (η) and dielectric permittivity (ϵ) are the two most important physicochemical parameters affecting the rate of the reactions in solutions. In the following paragraphs, the effect of these two factors will be discussed.

Effect of Viscosity. Radical reactions are often diffusion controlled, and our k values are close to the range that corresponds to that of diffusion-controlled reactions. Therefore, one can assume that the viscosity dependence of k should be inversely proportional to viscosity η,[26] that is, the $k\eta$ products should be constant. The $k\eta$ products for NOB and DMNA are plotted as a function of solvent composition in Figure 3. It is seen that the $1/\eta$ variation of k is valid only for limited ranges of solvent compositions. For DMNA this range is between 10 and 60 mol % MeOH, whereas for NOB $k\eta$ varies only slightly in the relatively wide composition range between 20 and 100 mol % MeOH. As concerns the viscosity dependence of the reaction of e_s^- with NO_2B,[21] which is also shown in Figure 3 for comparison, k varies as η^{-1} in only a small range of solvent compositions in the water rich side between 0 and 30 mol % MeOH and shows a weak viscosity dependence of $\eta^{-0.3}$ in the methanol rich region.

One can conclude that the variation of reaction rate constants of *o*-Ps or e_s^- in different solvents cannot be interpreted in terms of viscosity alone.

Dielectric Permittivity Effects. The other important solvent property that can affect the rate of the reactions, especially with

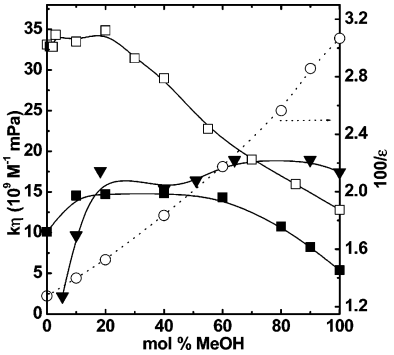

Figure 3. $k\eta$ products for the reactions of *o*-Ps with NOB (▼) and DMNA (■) at 20 °C and of e_s^- with NO_2B[21] at 25 °C (□) in MeOH−water mixtures. For comparison, the dependence of the dielectric permittivity ($1/\epsilon$, ○) on solvent composition is also shown. ϵ data are taken from ref 23. The lines are visual fits, to guide the eye.

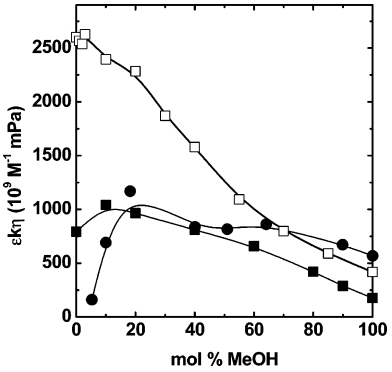

Figure 4. Rate constants double-normalized for dielectric permittivity and viscosity ($\epsilon k\eta$) for the reactions of *o*-Ps with NOB (●) and DMNA (■) at 20 °C and of e_s^- with NO_2B[21] (□) at 25 °C in MeOH−water mixtures. The static dielectric permittivity and viscosity data are taken from ref 23. The lines are visual fits, to guide the eye.

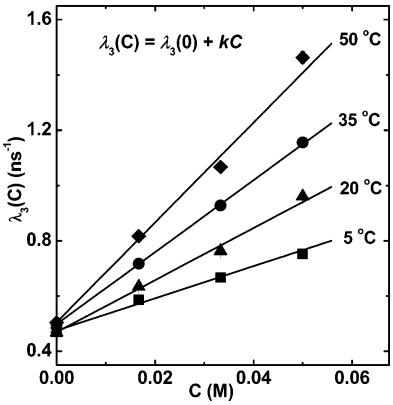

Figure 5. Decay rate constants of *o*-Ps atom (λ_3) as a function of DMNA concentration in a MeOH−water mixture containing 20 mol % MeOH at different temperatures: ■, 5 °C; ▲, 20 °C; ●, 35 °C; ♦, 50 °C. The slopes of the least-squares-fit lines (k) increase with increasing temperature.

polar solutes, is the solvent dielectric permittivity (ϵ). Considering the Debye equation,[27] one can expect $1/\epsilon$ dependence on the viscosity-normalized reaction rate constant $k\eta$. In the case of the reaction of e_s^- with NO_2B it was found[21] that the decrease of $k\eta$ with increasing $1/\epsilon$ in the methanol rich region is in the opposite direction to that expected. The variation of $1/\epsilon$ with solvent composition shown in Figure 3 clearly demonstrates this opposite trend.

Although *o*-Ps, in contradistinction to e_s^-, is a neutral particle, the effect of ϵ on the reactions of these two species may not differ fundamentally. As *o*-Ps and the polar solute diffuse together, the neutral particle will be strongly polarized by the dipole, and hence its electron will be directed toward the positively charged aromatic ring. Thus, the interaction of a highly polarized *o*-Ps atom and that of the solvated electron with a molecule with a dipole character can be treated in a similar way.

The plots for DMNA and NOB in Figure 3 are similar only in the water rich region of the solvent mixtures up to the viscosity maximum of the system. From then on with increasing MeOH content, the DMNA curve begins to drop whereas the NOB curve stays essentially constant. The trend of the plot for DMNA is similar to that for the reaction of e_s^- with NO_2B.[21] To explain the unexpected decrease of $k\eta$ with increasing $1/\epsilon$ the authors of ref 21 suggest that NO_2B is solvated by alcohol molecules oriented such that alkyl groups are adjacent to the benzene ring and hydroxyl groups adjacent to the nitro group and hence the nonpolar alkyl groups of the alcohol molecules inhibit the electron transport to the positive end of the polar solute which is the aromatic ring.

If the above interpretation is correct, one can conclude that the observed difference between DMNA and NOB should be attributed to their different solvation properties. NOB is, however, a molecule of more hydrophobic character than DMNA, which manifests itself in its very low solubility in water; hence, it can be more easily solvated by methanol molecules than DMNA. Thus, the observed difference between these two molecules and the decreasing trend of the $k\eta$ versus $1/\epsilon$ plots cannot be reasonably accounted for by solvation effects.

In order to separate the theoretically expected $1/\eta$ and $1/\epsilon$ effects from the effect of the solvent structure, it seems reasonable to present the rate constants double normalized both for dielectric permittivity and viscosity in the form of $\epsilon k\eta$.[28] One can assume that such a type of plot might reflect dominantly the effect of structural changes in the medium. Our double-normalized rate constants ($\epsilon k\eta$) together with the similar data for the reaction of e_s^- with NO_2B[21] are shown in Figure 4. The NO_2B curve monotonically decreases from water to MeOH. The curves for NOB and DMNA, on the other hand, exhibit maxima at a solvent composition of about 10−20 mol % MeOH content and from then on decline monotonically to pure MeOH. The numerical values of the double-normalized rate constants in MeOH are very close to each other in all three cases, whereas in water they differ significantly.

The $\epsilon k\eta$ plots for NOB and DMNA have similar curvature to those found for the activation parameters of the *o*-Ps reaction with DMNA (Figures 7 and 9), and a possible explanation for the appearance of the maxima will be given later in the paragraph discussing the activation enthalpy results.

Temperature Dependence. The temperature dependence of the reactions of *o*-Ps with DMNA has been measured at five solvent compositions of the MeOH−water mixtures in the temperature range of 5−50 °C. As an illustration, Figure 5 shows the decay rate constants of *o*-Ps (λ_3) plotted as a function of DMNA concentration at different temperatures in a MeOH−water mixture containing 20 mol % MeOH. The slope of the least-squares-fit lines, that is, the rate constant (k) of the *o*-Ps reaction with DMNA, increases with increasing temperature. This was the observed trend at other solvent compositions too. In contradistinction to the case of DMNA, the rate of the reaction of *o*-Ps with *t*-NOBu in MeOH was not affected by increasing temperature and its value remained constant within experimental error over the entire temperature range of 5−60 °C.

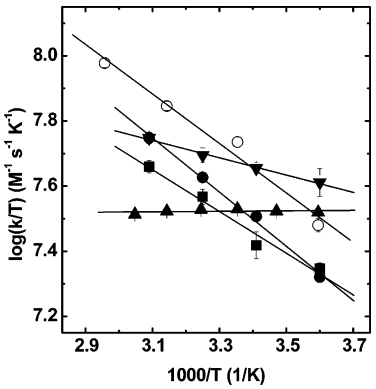

Figure 6. Log k/T vs $1/T$ Arrhenius plots for the reaction of *o*-Ps with DMNA in different MeOH−water mixtures: ○, 0; ●, 20; ■, 40; ▼, 80; ▲, 100 mol % MeOH. The parameters of the least-squares-fit lines, i.e., the average activation entropies ($\Delta S^{\ddagger}$) and enthalpies ($\Delta H^{\ddagger}$) are presented in Table 2 and plotted as a function of solvent composition in Figures 7 and 9.

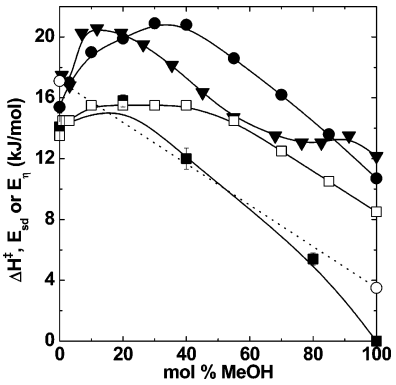

Figure 7. Solvent composition dependence of the average activation enthalpy ($\Delta H^{\ddagger}$) for the reaction of *o*-Ps with DMNA (■) and HTMPO (○); the average activation enthalpy of the reaction of e_s^- with NO_2B (□); the activation energy of the solvent viscosity (E_{η}, ●); the activation energy of the self-diffusion (E_{sd}, ▼) of the MeOH molecules in MeOH−water mixtures. $\Delta H^{\ddagger}$ for HTMPO and NO_2B, E_{η}, and E_{sd} values were calculated from data in refs 15, 21, 23, and 29, respectively. The lines are visual fits, to guide the eye.

Activation Parameters. The activation parameters of the reactions have been calculated from the Arrhenius law (eq 2), where $\Delta H^{\ddagger}$and $\Delta S^{\ddagger}$ are the average activation enthalpy and activation entropy, respectively:

$$k/T = R/(N_A h) \exp(\Delta S^{\ddagger}/R) \exp(-\Delta H^{\ddagger}/RT) \qquad (2)$$

The log(k/T) versus $1/T$ variations for DMNA in different MeOH−water mixtures are presented in Figure 6. The activation parameters obtained from the least-squares fits of the data to the linearized Arrhenius law are presented in Table 2 and plotted as a function of solvent composition in Figures 7 and 9.

Activation Enthalpies. $\Delta H^{\ddagger}$ values for the reaction of *o*-Ps with DMNA are plotted as a function of solvent composition in Figure 7. For comparison, $\Delta H^{\ddagger}$ values for the reactions of *o*-Ps with HTMPO and e_s^- with NO_2B, activation energies of the solvent viscosity (E_{η}) and of the self-diffusion (E_{sd}) of MeOH molecules are also shown in Figure 7. ($\Delta H^{\ddagger}$ for HTMPO and NO_2B, E_{η}, and E_{sd} values were calculated from data in refs 15, 21, 23, and 29, respectively.)

The variations of the activation parameters with solvent composition presented in Figures 7 and 9 are qualitatively similar to those of the activation energies of solvent viscosity (E_{η}), the self-diffusion (E_{sd}) of methanol molecules,[29] and the activation enthalpy of the reaction of e_s^- with NO_2B.[21] However, the measured values of the average activation enthalpy ($\Delta H^{\ddagger}$) for both the *o*-Ps and the e_s^-reactions are lower in the whole composition range than the activation energies of the solvent viscosity and that of the self-diffusion of the MeOH molecules.

The $\Delta H^{\ddagger}$ of the reactions of *o*-Ps exhibits a maximum in solutions containing about 20 mol % MeOH. The curve for the activation energy of the reaction of e_s^- with NO_2B shows a similar curvature, however, with a less pronounced maximum. The appearance of this maximum can be reasonably well explained in a qualitative fashion by Samoilov's theory about the structure of alcohol−water mixtures.[30] According to this theory, the increasing alcohol content increases the stability of the mixture by filling up the free volume sites of the hydrogen-bonded structure of water with alcohol molecules. Higher alcohol content, on the other hand, destroys the hydrogen-bonded structure of water. The composition of maximum stability depends on the size of the alcohol molecule. For methanol, this particular composition is around 20 mol % MeOH. Thus, the highest values of activation energies for all types of transport processes are expected to occur in the same concentration region corresponding to the most rigid solvent structure. Our results are in accord with this qualitative picture.

It is worth mentioning that the main features of the reaction of e_s^- with carbon tetrachloride in ethanol−water mixtures[31] are very similar to those of the reaction of *o*-Ps with DMNA in MeOH−water mixtures. The activation energy curve of the former reaction has a shape similar to that for self-diffusion in the binary mixture. Both curves exhibit maxima, which coincide with the mole fractions at which the extremes in the excess heat of mixing function occurs. (See Figure 2 in ref 31.)

Moreover, as is seen in Figure 4, the double-normalized rate constants ($\epsilon k\eta$) also exhibit extremes at the concentration range of maximum stability of the mixtures; hence, these curves may also reflect the structural changes in the medium. It is, however, not clear why both the reaction rates and the activation energies have extremes at the most stable or most rigid solvent composition.

Anderton and Kauffman in their paper on dielectric-dependent activation energies of photoisomerization rates in *n*-alcohols[32] pointed out that one might expect the activation energy (E_a) of the reaction to exhibit an "Onsager reaction field" type dependence on solvent permittivity, given by eq 3.

$$E_a \propto (\epsilon - 1)/(\epsilon + 2) \qquad (3)$$

We have tested the suggested dielectric permittivity effect. It is clearly seen in Figure 8 that the $\Delta H^{\ddagger}$ values for the reactions of *o*-Ps with DMNA and of e_s^- with NO_2B plotted as a function of solvent composition exhibit very similar trends to that for the $(\epsilon - 1)/(\epsilon + 2)$ values in the composition range from pure MeOH up to the concentration corresponding to the most stable solvent structure. In the water rich region, however, the activation enthalpy values are smaller than expected from the permittivity dependence.

Activation Entropies. The solvent composition dependence of the average activation entropy ($\Delta S^{\ddagger}$) of the *o*-Ps reaction with DMNA and HTMPO[15] are shown in Figure 9 together with the data for the reaction of e_s^- with NO_2B.[21] $\Delta S^{\ddagger}$ for DMNA exhibits a maximum also at that particular solvent composition which corresponds to the most ordered structure. Small positive activation entropies have been measured in water and in the mixture containing 20 mol % MeOH. After the maximum, $\Delta S^{\ddagger}$ decreases and becomes more and more negative with increasing

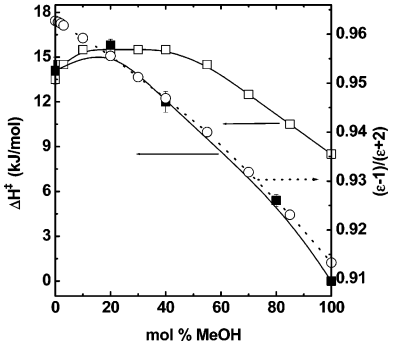

Figure 8. $(\epsilon - 1)/(\epsilon + 2)$ values plotted against solvent composition (○, dotted line) exhibiting an "Onsager reaction field" type dependence on solvent permittivity of the activation enthalpy ($\Delta H^{\ddagger}$) in MeOH−water mixtures. (■, reaction of *o*-Ps with DMNA; □, reaction of e_s^- with NO_2B[21]). ϵ data are taken from ref 23. The lines are visual fits, to guide the eye.

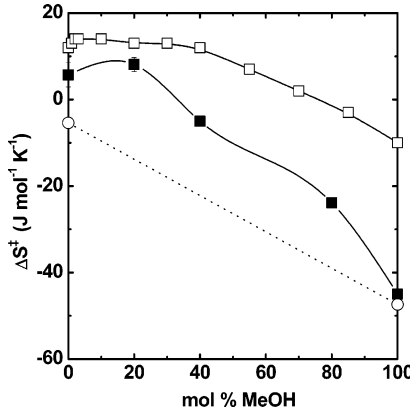

Figure 9. Solvent composition dependence of the average activation entropy ($\Delta S^{\ddagger}$) of the reaction of *o*-Ps with DMNA (■) and HTMPO (○) and of the reaction of e_s^- with NO_2B (□) in MeOH−water mixtures. $\Delta S^{\ddagger}$ values for HTMPO were calculated from data taken from ref 15 and those for NO_2B from data taken from ref 21. The lines are visual fits, to guide the eye.

MeOH content. A maximum, although less pronounced, appears also for the reaction of e_s^- with NO_2B, and $\Delta S^{\ddagger}$ for HTMPO also has a much higher negative value in MeOH than in water.

According to the theory,[33] the value of $\Delta S^{\ddagger}$ can be influenced either by the change in the degree of solvation or by the solvent polarity. If the activated complex is solvated more extensively than the reactant, it implies a lowering of the entropy. The value of $\Delta S^{\ddagger}$ in a polar solvent is usually a smaller negative number than in an apolar solvent. In the latter case, the formation of the solvation shell represents an appreciable increase in ordering, whereas the polar solvent is already well ordered, and no marked change will take place for solvation. For this reason, to reach the transition state in less polar solvents the entropy must decrease more than in more polar ones.[33] Thus, the observed trends of the solvent composition dependence of $\Delta S^{\ddagger}$ can be reasonably well accounted for by the decreasing polarity of the mixtures with increasing MeOH content. The positive numerical values of $\Delta S^{\ddagger}$ in the water rich region suggest that the structure of the activated complex is less ordered than the extremely rigid solvent structure around the reactants. Then with increasing MeOH content both the ordering of the structure and the solvent polarity decrease resulting in increasingly larger negative values of $\Delta S^{\ddagger}$.

Isokinetic Relations. If for a series of reactions, for example, for the same reaction in different solvents, the mechanism of the reactions is the same, a linear relationship is expected

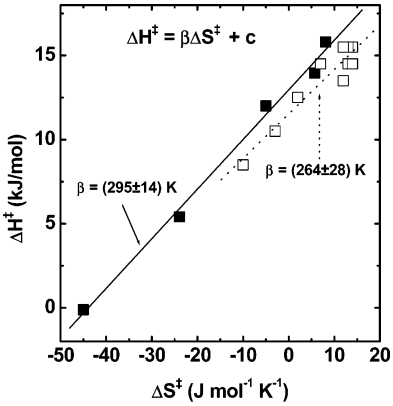

Figure 10. Average activation enthalpies ($\Delta H^{\ddagger}$) plotted as a function of average activation entropies ($\Delta S^{\ddagger}$) exhibit the isokinetic relation for the reactions of *o*-Ps with DMNA (■, solid line) and of e_s^- with NO_2B (□, dotted line) in MeOH−water mixtures. Data for NO_2B were taken from ref 21. The lines are the results of least-squares fits of the data to eq 4.

between the activation entropy and the activation enthalpy. This relationship is the so-called isokinetic relation:[34]

$$\Delta H^{\ddagger} = \beta \Delta S^{\ddagger} + c \qquad (4)$$

Here, β is the isokinetic temperature and c is a constant. At $T_{ik} = \beta$ the rate constants are equal for the reactions of the series: $k(T_{ik}) = k_{ik}$. Thus, the isokinetic rate constant does not depend on the activation parameters of the individual reactions, that is, on the solvent.

The isokinetic relation has proved to be valid for both the reactions of *o*-Ps with DMNA and of e_s^- with NO_2B[21] (Figure 10). The fitted values of the isokinetic temperature are $\beta = 295 \pm 14$ K and $\beta = 264 \pm 28$ K for DMNA and NO_2B, respectively. Thus, we can conclude that the mechanisms of both reactions are independent of solvent composition in the MeOH−water system.

Conclusions

The reactions of *o*-Ps with nitroso spin traps are nearly diffusion controlled. The reactivity of the solutes toward *o*-Ps is determined by their LUMO energies. The nucleophilic *o*-Ps attacks the molecules at their electron deficient aromatic ring.

The analysis of the experimental results shows that the k versus $1/\eta$ relationship is an insufficient criterion for diffusion-controlled reactions in nonideal solvent mixtures. Similar deviations from the expected k versus $1/\epsilon$ relationship are observed too. The effect of solvent structure on the reaction rates is more reliably reflected by the solvent dependence of the double-normalized rate constants $\epsilon k \eta$.

The activation enthalpies of the diffusion-controlled reactions of *o*-Ps with DMNA reflect the change in the solvent structure as a function of the composition of the binary mixtures. The composition corresponding to the maximum value of $\Delta H^{\ddagger}$ coincides with the mole fraction at which the maxima for the activation energies of viscosity and self-diffusion occur. $\Delta H^{\ddagger}$ exhibits an "Onsager reaction field" type $(\epsilon - 1)/(\epsilon + 2)$ dependence on solvent permittivity.

Although the rate constants depend on the solvent composition in a complex and solute-dependent manner, the validity of the isokinetic relation between $\Delta H^{\ddagger}$ and $\Delta S^{\ddagger}$ shows that the mechanism of the reactions of *o*-Ps is independent of the solvent composition in methanol−water mixtures.

When the reaction of *o*-Ps with DMNA to the reaction of e_s^- with NO_2B in MeOH−water mixed solvents is compared, similar trends are observed in many cases especially for the solvent and dielectric permittivity dependence of the activation parameters.

Acknowledgment. The authors are grateful to Dr. G. Duplâtre for stimulating discussions. They are also much indebted to Mrs. G. Bor for her valuable technical assistance. This work was financially supported by the Hungarian Scientific Research Fund (OTKA Grant T037592).

References and Notes

(1) Lévay, B. *At. Energy Rev.* **1979**, *17*, 413.
(2) *Positron and Positronium Chemistry*; Schrader, D. M., Jean, Y. C., Eds.; Elsevier: Amsterdam, 1988.
(3) Mogensen, O. E. *Positron Annihilation in Chemistry*; Springer-Verlag: Berlin, 1995.
(4) Mogensen, O. E. *J. Chem. Phys.* **1974**, *60*, 998.
(5) Shantarovich, V. P.; Goldanskii, V. I.; Shantarovich, P. S.; Koldaeva, O. V. *Dokl. Akad. Nauk SSSR* **1971**, *197*, 1121.
(6) Madia, W. J.; Nicholas, A. L.; Ache, H. J. *J. Appl. Phys.* **1974**, *3*, 189.
(7) Goldanskii, V. I.; Shantarovich, V. P. *Appl. Phys.* **1974**, *3*, 335.
(8) Madia, W. J.; Nicholas, A. L.; Ache, H. J. *J. Am. Chem. Soc.* **1975**, *97*, 5041.
(9) Bartal, L. J.; Ache, H. J. *J. Phys. Chem.* **1973**, *77*, 2060.
(10) Lévay, L.; Lévay, B.; Vértes, A. *Chem. Phys.* **1988**, *124*, 155.
(11) Goldanskii, V. I.; Shantarovich, V. P. *Appl. Phys.* **1974**, *3*, 335.
(12) Aravin, L. G.; Sobolev, B. V.; Shantarovich, V. P. *High Energy Chem. (Engl. Transl.)* **1973**, *7*, 467.
(13) Goldanskii, V. I.; Shantarovich, V. P.; Shishkin, A. V.; Tatur, A. O. *Dokl. Phys. Chem. (Engl. Transl.)* **1976**, *229*, 750.
(14) Shantarovich, V. P.; Jansen, P. *Chem. Phys.* **1978**, *34*, 39.
(15) Abbé, J. Ch.; Duplâtre, G.; Haessler, A.; Marques Netto, A.; Pilo Veloso, D. *J. Phys. Chem.* **1984**, *88*, 2071.
(16) Keana, J. F. W. *Chem. Rev.* **1977**, *78* (8), 37.
(17) Lagercrantz, C. *J. Phys. Chem.* **1971**, *75*, 3466.
(18) Franks, F.; Ives, D. J. G. *Q. Rev.* **1966**, *20*, 1.
(19) Milosavljević, B. H.; Mićić, O. I. *Phys. Chem.* **1978**, *82*, 1359.
(20) Maham, Y.; Freeman, G. R. *J. Phys. Chem.* **1988**, *92*, 1506.
(21) Lai, Ch. C.; Freeman, G. R. *J. Phys. Chem.* **1990**, *94*, 302.
(22) Lai, Ch. C.; Freeman, G. R. *J. Phys. Chem.* **1990**, *94*, 4891.
(23) Timmermans, J. *Physico-Chemical Constants of Binary Mixtures*; Interscience: New York, 1960; Vol. 4.
(24) Kirkegard, P.; Eldrup, M.; Mogensen, O. E.; Pedersen, N. J. *Comput. Phys. Commun*. **1981**, *23*, 307.
(25) Frisch, M. J.; Trucks, G. W.; Schlegel, H. B.; Scuseria, G. E.; Robb, M. A.; Cheeseman, J. R.; Zakrzewski, V. G.; Montgomery, J. A., Jr.; Stratmann, R. E.; Burant, J. C.; Dapprich, S.; Millam, J. M.; Daniels, A. D.; Kudin, K. N.; Strain, M. C.; Farkas, O.; Tomasi, J.; Barone, V.; Cossi, M.; Cammi, R.; Mennucci, B.; Pomelli, C.; Adamo, C.; Clifford, S.; Ochterski, J.; Petersson, G. A.; Ayala, P. Y.; Cui, Q.; Morokuma, K.; Malick, D. K.; Rabuck, A. D.; Raghavachari, K.; Foresman, J. B.; Cioslowski, J.; Ortiz, J. V.; Stefanov, B. B.; Liu, G.; Liashenko, A.; Piskorz, P.; Komaromi, I.; Gomperts, R.; Martin, R. L.; Fox, D. J.; Keith, T.; Al-Laham, M. A.; Peng, C. Y.; Nanayakkara, A.; Gonzalez, C.; Challacombe, M.; Gill, P. M. W.; Johnson, B. G.; Chen, W.; Wong, M. W.; Andres, J. L.; Head-Gordon, M.; Replogle, E. S.; Pople, J. A. *Gaussian 98*, revision A.1; Gaussian, Inc.: Pittsburgh, PA, 1998.
(26) Umberger, J. Q.; LaMer, V. K. *J. Am. Chem. Soc.* **1945**, *67*, 1099.
(27) Debye, P. *Trans. Electrochem. Soc.* **1942**, *82*, 265.
(28) Senanayake, P. C.; Freeman, G. R. *J. Chem. Phys.* **1987**, *87*, 7007.
(29) Erdey-Grúz, T.; Fodorné Csányi, P.; Lévay, B.; Szilágyiné Győri, E. *Acta Chim. Acad. Sci. Hung.* **1971**, *69*, 423.
(30) Bulaeva, M. N.; Samoilov, O. Ja. *Zh. Strukt. Khim.* **1963**, *4*, 502.
(31) Mićić, O. I.; Čerček, B. *J. Phys. Chem.* **1977**, *81*, 833.
(32) Anderton, R. M.; Kauffman, J. F. *J. Phys. Chem.* **1994**, *98*, 12125.
(33) Ruff, F.; Csizmadia, I. G. *Organic Reactions, Equilibria, Kinetics and Mechanism;* Elsevier: Amsterdam, 1994; Chapter 6.
(34) Leffler, J. E. *J. Org. Chem.* **1955**, *20*, 1202.